Mon. Not. R. Astron. Soc. **379,** 1498–1506 (2007) doi:10.1111/j.1365-2966.2007.12042.x

MOST⋆ photometry of the RRd Lyrae variable AQ Leo: two radial modes, 32 combination frequencies and beyond

Michael Gruberbauer,[1]† Katrien Kolenberg,[1,2] Jason F. Rowe,[3] Daniel Huber,[1] Jaymie M. Matthews,[3] Piet Reegen,[1] Rainer Kuschnig,[3] Chris Cameron,[3] Thomas Kallinger,[1] Werner W. Weiss,[1] David B. Guenther,[4] Anthony F. J. Moffat,[5] Slavek Rucinski,[6] Dimitar Sasselov[7] and Gordon A. H. Walker[3]

[1]*Institute of Astronomy, University of Vienna, Türkenschanzstrasse 17, A-1180 Vienna, Austria*
[2]*Institute of Astronomy, University of Louvain, Celestijnenlaan 200D, B-3001 Heverlee, Belgium*
[3]*Department of Physics & Astronomy, University of British Columbia, 6224 Agricultural Road, Vancouver, BC V6T 1Z1, Canada*
[4]*Department of Astronomy and Physics, St. Mary's University, Halifax, NS B3H 3C3, Canada*
[5]*Département de physique, Université de Montréal, Montréal, QC H3C 3J7, Canada*
[6]*David Dunlap Observatory, Department of Astronomy, University of Toronto, Toronto, ON L4C 4Y6, Canada*
[7]*Harvard-Smithsonian Centre for Astrophysics, Cambridge, MA 02138, USA*

Accepted 2007 May 30. Received 2007 May 30; in original form 2007 April 16

ABSTRACT

Highly precise and nearly uninterrupted optical photometry of the RR Lyrae star AQ Leo was obtained with the MOST (Microvariability and Oscillations of Stars) satellite over 34.4 d in 2005 February–March. AQ Leo was the first known double-mode RR Lyrae pulsator (RRd star). Three decades after its discovery, MOST observations have revealed that AQ Leo oscillates with at least 42 frequencies, of which 32 are linear combinations (up to the sixth order) of the radial fundamental mode and its first overtone. Evidence for period changes of these modes is found in the data. The other intrinsic frequencies may represent an additional non-radial pulsation mode and its harmonics (plus linear combinations) which warrant theoretical modelling. The unprecedented number of frequencies detected with amplitudes down to mmag precision also presents an opportunity to test non-linear theories of mode growth and saturation in RRd stars.

Key words: methods: data analysis – methods: statistical – stars: individual: AQ Leo – stars: oscillations – stars: variables: other.

1 INTRODUCTION

The human part of the history of AQ Leo ($V \sim 12.6$) begins with its classification as a variable of the RW Aurigae type by Hoffmeister (1944) at the Sonneberg Observatory. 15 yr later, Wenzel (1961) concluded that the star is an RR Lyrae pulsator with a strongly variable light curve. Jerzykiewicz & Wenzel (1977, hereafter JW77) thoroughly analysed their photometry gathered during 1973–1975 to recognize for the first time that AQ Leo is a double-mode RR Lyrae star. They identified the prototype of the class. Jerzykiewicz, Schult & Wenzel (1982, hereafter JSW82) later re-evaluated the data and their comparisons to earlier archived exposures raised the possibility of a period change in the early 1970s. In the meantime, double-mode RR Lyraes, designated RRd stars, have been identified in globular clusters, dwarf spheroidal galaxies, the Magellanic Clouds and the Galactic field (see e.g. Clement, Kinman & Suntzeff 1991).

RRd stars pulsate in a combination of first overtone and fundamental radial modes. The ratio of the first overtone to the fundamental period is about 0.74–0.75 (see e.g. Alcock et al. 2000). Usually the amplitude of the first overtone is stronger, but not always so (e.g. Oaster, Smith & Kinemuchi 2006). RRd variables are particularly important because their double-mode nature affords an opportunity to determine their masses based on the period ratio, largely independently of stellar evolution theory, and hence to a much higher precision than is possible for monomode RR Lyrae stars (Kovács, Buchler & Marom 1991).

AQ Leo happens to fall in the field around a MOST (Microvariability and Oscillations of Stars) space mission primary science target, ι Leo. This alignment presented an ideal opportunity to obtain the first new light curve of this star in three decades, with very complete time coverage and unequalled photometric precision. The long time baseline between the JW77 photometry and the MOST observations is well suited to search for period changes in AQ Leo. The precision of the MOST photometry means that the amplitude

⋆MOST is a Canadian Space Agency mission, jointly operated by Dynacon Inc., the University of Toronto Institute for Aerospace Studies and the University of British Columbia, with the assistance of the University of Vienna.
†E-mail: gruberbauer@astro.univie.ac.at

© 2007 The Authors. Journal compilation © 2007 RAS

ratio of the two modes can be measured more accurately than before; however, in the MOST custom passband, not in a standard filter system. If AQ Leo is re-observed by MOST in the future, it will be possible to test theoretical predictions of mode switching in RRd stars. The sampling and precision of the MOST photometry also make it possible to search for *non-radial* modes in an RRd star with a sensitivity that cannot be achieved in ground-based data.

2 MOST PHOTOMETRY

The MOST space mission was designed to obtain high-precision optical photometry of bright stars, monitored for weeks at a time with high duty cycle and time sampling of at least once per minute (Walker et al. 2003). MOST is a microsatellite housing a 15-cm Maksutov telescope feeding a CCD photometer through a single custom broad-band filter (350–700 nm). Its polar Sun-synchronous orbit allows it to observe stars in its continuous viewing zone for up to two months without interruption.

AQ Leo was observed by MOST satellite in the same field as its primary science target ι Leo, for 34.434 d during 2005 February 14 to March 22 (HJD 245 3416.671–245 3451.105). One of the faintest stars ever observed by MOST at $V \sim 12.6$, AQ Leo was a Direct Imaging target. Direct Imaging is the MOST observing mode where a defocused star image is projected on to an open area of the science CCD (see Rowe et al. 2006a). The star is sampled within a 20×20 pixel subraster of the CCD and photometry is extracted through aperture methods and PSF (point spread function) fitting of the image profile. The exposure time was 25 s and exposures were made every 30 s. The data were reduced independently by two of the authors, JFR at University of British Columbia (UBC) and DH at Institute of Astronomy (IfA), Vienna, and the results then compared.

The UBC MOST Direct Imaging photometry reduction pipeline is similar to the treatment of ground-based CCD photometry in that it measures the stellar flux though a combination of an aperture of pixels centred on the star and fitting of its PSF image profile. To minimize the effects of pointing errors on the photometry, dark and flat-field corrections were performed by monitoring individual pixel responses during test exposures on fields empty of stars brighter than the background. The correlation in the raw photometry between the instrumental magnitude light curve and the estimated sky background was removed as described in Rowe et al. (2006a).

The IfA Vienna reduction was based on a pixel-to-pixel decorrelation technique developed by Reegen et al. (2006) for MOST Fabry Imaging photometry. To define a fixed aperture mask by which pixels illuminated by the star and by the background can be identified, the PSFs of the star on all subraster images must be aligned. This is not the case in the raw images due to minor pointing errors during the observing run. As a first step, the centroid position of the stellar PSF for each image is computed. Subsequently, all other pixel intensities relative to the centroid coordinates are computed by two-dimensional linear interpolation. Finally, all pixels of each image are shifted by integer values in x and y to a pre-defined centre position. Since this shifting process decreases the resulting image size common to all exposures, frames suffering from pointing errors larger than 3 pixel (about 9 arcsec) from the subraster centre are rejected. (This pointing threshold eliminated 7 per cent of all the exposures in the raw AQ Leo time series.) Once all the images are aligned, the decorrelation can be computed to reduce the background effects of modulated stray light.

Both reductions led to consistent light curves and frequency identifications. The IfA light curve has higher point-to-point scatter than the UBC reduction, and the UBC reduction is presented here as the AQ Leo light curve. However, both light curves were searched independently by the frequency analysis techniques described in the next section, and the results are consistent for both reductions. The final duty cycle of the reduced photometry is 82 per cent. The reduced light curve is presented in Fig. 1. The AQ Leo raw data and reduced light curve are available in the MOST Public Data Archive, accessed via the science page of the MOST web site www.astro.ubc.ca/MOST

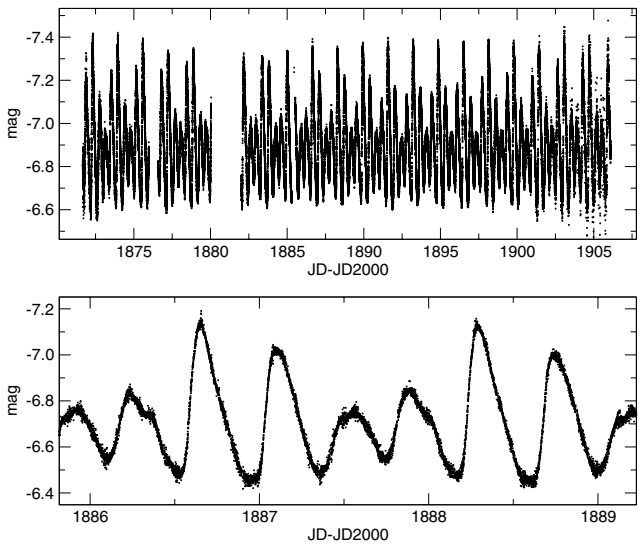

Figure 1. The light curve of AQ Leo obtained by MOST. The entire time series (upper panel), as well as an expanded view of 3.7 d of the light curve (lower panel).

3 FREQUENCY ANALYSIS

Frequency analyses of the MOST AQ Leo light curve were performed independently with three different routines: PERIOD04 (Lenz & Breger 2005), SIGSPEC (Reegen 2007) and non-linear least squares fitting and bootstrapping (Rowe et al. 2006b; see also Cameron et al. 2006), and the results compared to ensure that only significant intrinsic stellar frequencies were identified.

3.1 PERIOD04

PERIOD04 (Lenz & Breger 2005) is a routine which applies a single-frequency power spectrum and simultaneous multifrequency sine-wave fitting. The program includes advanced options such as the calculation of optimal light curve fits for multiperiodic signals including harmonics, combination frequencies and combs of equally spaced frequencies. In this analysis, we identified frequencies through successive pre-whitening. As each new significant frequency was added to the fit, the optimum values of first overtone frequency f_1 and the fundamental f_0, and their amplitudes and phases, were determined by minimizing the residual rms error of the fit. After no additional frequencies were detected in the data, we applied a simultaneous least-squares fit of all the independent frequencies and their significant linear combinations, as well as all amplitudes and phases. This included a final optimization of the first overtone and radial fundamental frequencies.

Besides determining the uncertainties from the error matrix of a least-squares calculation and/or from analytically derived formulae, PERIOD04 also provides an interface for estimating the uncertainties

of the fit parameters by means of Monte Carlo simulations. A set of time series is generated for which the times are the same as for the original time series, and for which the magnitudes (intensities) are calculated from those predicted by the last fit plus Gaussian noise. A least-squares calculation is made for every time string, and the resulting uncertainties are based on the distribution of the fit parameters.

3.2 Non-linear least-squares fitting and bootstrapping

The non-linear least-squares approach we used for determining the sinusoid parameters from the AQ Leo time series follows the philosophy of PERIOD04 (Lenz & Breger 2005) described above. Discrete Fourier transforms (DFTs) are calculated and an updated fit is subtracted from the data successively, until there is no meaningful change in the fit residuals. The data are fit using an equation of the form

$$\mathrm{mag} = A_0 + \sum_{j=1,n} A_j \cos(2\pi f_j t - \theta_j), \quad (1)$$

where A_0 is a linear offset and f_j, A_j and θ_j are the frequency, amplitude and phase for each successive peak found in the amplitude spectrum. The uncertainties calculated for time series parameters derived from non-linear least-squares fitting depend on the noise of the data (which may be a combination of instrumental and random processes) and on the time sampling.

It is also known that fitted phase and frequency parameters are correlated, leading to underestimated uncertainties in these parameters when calculated from a covariance matrix (see e.g. Montgomery & O'Donoghue 1999). The 'bootstrap' (see Wall & Jenkins 2003) is a very effective way to assess the uncertainties in these fitted parameters. The procedure has recently been used in a number of MOST applications (see e.g. Cameron et al. 2006; Rowe et al. 2006b; Saio et al. 2006). Clement, Jankulak & Simon (1992) also used a bootstrap to estimate the uncertainties in Fourier parameters they derived for RR Lyrae stars. Bootstrapping produces a distribution for each calculated parameter by constructing a large number of light curves from the original data. No assumptions must be made about noise properties of the data and individual photometric errors are not required for the calculations. Each new light curve is assembled by randomly selecting N points from the original light curve (also containing N points) with the possibility of replacement. The new synthetic light curves preserve the noise properties of the original data. The fit is repeated for each new light curve, eventually building distributions in each of the fit parameters. We then estimate the 1σ error bars from the analytic expression for the standard deviation of each distribution under the assumption that they are normally distributed. Each distribution is checked to ensure this assumption is valid. The uncertainties are listed in Table 1 and give consistent answers with SIGSPEC, as described below. We point out that bootstrapping only estimates the uncertainties in parameters. It does not refine the parameter values or assign significances to them.

3.3 SIGSPEC and background correction

A third independent frequency search was performed, where the statistical significances of peaks in the DFT of the AQ Leo light curve were estimated through SIGSPEC (Reegen 2007). This routine calculates an unbiased false alarm probability (based on white noise) associated with the amplitude of a peak in Fourier space. It produces a significance spectrum containing all frequencies above a certain threshold in significance, as determined by successive prewhitening.

The analyses above identify frequencies present in the data with high statistical significance and signal-to-noise ratio, but some of these may be due to background variations in the data, not intrinsic to the star. The frequencies of some background artefacts in MOST data are known; e.g. the orbital frequency of the satellite and its harmonics, at which stray light modulation is observed. We carried out tests to distinguish periodic effects in the background from intrinsic stellar signal. We did this by analysing not only the variation of the mean integrated intensity within an aperture surrounding the star ('stellar signal', which includes the background in those pixels) but also the mean integrated intensity outside a larger aperture which includes the outermost pixels of the CCD subraster ('background signal'). Since our three independent frequency analyses yield consistent results, we chose to use the list of frequencies, amplitudes and phases from SIGSPEC to compare the significance spectra of the stellar signal light curve and the background signal light curve.

First, peaks from the stellar signal DFT and the background DFT are flagged if their frequencies agree within the uncertainty. Based on extensive numerical simulations, Kallinger, Reegen & Weiss (2007) found the upper limit for the frequency uncertainty in a time series to be

$$\Delta f = \frac{1}{\Delta T \sqrt{\mathrm{sig}(A, f, \theta)}}, \quad (2)$$

where ΔT is the total data set length in days and sig (A, f, θ) is the spectral significance for a given amplitude, frequency and phase, as defined in Reegen (2007). This upper limit on frequency uncertainty is more conservative (≈four times larger) than the value for the frequency error estimated by Montgomery & O'Donoghue (1999), based on an analytical solution for the error of a least-squares fit of a sinusoidal signal. If more than one coincident background peak is found around a given stellar peak within the frequency resolution, then the background peak with the highest significance is used for comparison to obtain the most conservative (and presumably the safest) solution.

Next, assuming stray-light-induced artefacts are additive in terms of their intensities, the peak amplitudes found to be significant in the background are rescaled from the mean background signal level to the mean stellar signal level in order to make the relative amplitudes (and hence the significances) comparable. Now, with the amplitude and spectral significance of a stellar Fourier peak and the rescaled amplitude and spectral significance of its coincident background peak, the 'conditional probability' that the stellar peak is not induced by background is calculated. The false alarm probability is transformed into a conditional spectral significance, and only those stellar peaks for which this is above 5.46 (corresponding roughly to an amplitude ratio of 4 for the target peak and the rescaled background peak) survive the cut. A detailed publication on this method, dubbed CINDERELLA (Comparison of Independent Relative Least-Squares Amplitudes), is in preparation (Reegen et al. 2007).

Uncertainties in frequency, amplitude and phase were first estimated through the relations of Montgomery & O'Donoghue (1999) and also approximated according to Kallinger et al. (2007). The resulting uncertainties are consistent with the bootstrap values described above, except where two frequencies are close to the resolution limit. In these cases, which apply to only four pairs of identified frequencies, the least-squares fitting can be perturbed, adding further small systematic errors added to the fitted values.

Table 1. Frequencies identified in AQ Leo from the MOST photometry by SIGSPEC, which are consistent with the other frequency analysis techniques described in the text. Amplitudes, phases, significances and uncertainties (derived by bootstrapping) are also listed. The phases correspond to epoch JD 2000 = JD 245 1545.

Id			f	σ_f	A	σ_A	Sig.	θ	σ_θ	Comb. err.
–	f_1	–	2.43 821	0.00 001	204.3	0.106	11 982	−1.855	0.001	0.00 000
–	$2f_1$	–	4.87 673	0.00 004	46.4	0.102	5 931	1.246	0.005	0.00 031
–	$3f_1$	–	7.31 515	0.00 013	16.6	0.101	2 502	−2.417	0.014	0.00 052
–	$4f_1$	–	9.75 228	0.00 064	5.4	0.118	521	−2.855	0.069	−0.00 056
–	$5f_1$	–	12.18 890	0.00 188	0.8	0.103	16	2.344	0.141	−0.00 215
f_0	–	–	1.81 896	0.00 002	113.5	0.098	10 702	1.612	0.002	0.00 000
$2f_0$	–	–	3.63 822	0.00 019	16.3	0.105	2 780	2.777	0.022	0.00 030
$3f_0$	–	–	5.45 637	0.00 098	3.3	0.120	203	2.703	0.113	−0.00 051
f_0	f_1	–	4.25 723	0.00 004	50.1	0.099	5 001	2.596	0.005	0.00 006
$-f_0$	f_1	–	0.61 923	0.00 005	45.5	0.120	8 321	−1.097	0.006	−0.00 002
f_0	$2f_1$	–	6.69 543	0.00 010	21.0	0.104	3 268	2.507	0.011	0.00 005
$-f_0$	$2f_1$	–	3.05 758	0.00 034	10.6	0.108	1 392	1.245	0.038	0.00 012
f_0	$3f_1$	–	9.13 385	0.00 025	9.0	0.103	1 304	−2.346	0.028	0.00 026
$-f_0$	$3f_1$	–	5.49 405	0.00 288	1.3	0.115	38	1.066	0.305	−0.00 162
f_0	$4f_1$	–	11.56 975	0.00 053	3.9	0.105	275	1.323	0.059	−0.00 205
$-f_0$	$4f_1$	–	7.93 297	0.00 103	2.3	0.115	104	−2.354	0.129	−0.00 091
$-f_0$	$5f_1$	–	10.37 055	0.00 225	1.2	0.104	32	3.033	0.210	−0.00 154
$2f_0$	f_1	–	6.07 720	0.00 021	10.6	0.102	1 503	−0.727	0.025	0.00 107
$2f_0$	$-f_1$	–	1.19 802	0.00 039	5.9	0.107	604	2.930	0.048	−0.00 169
$2f_0$	$2f_1$	–	8.51 455	0.00 023	10.5	0.103	1 606	1.244	0.024	0.00 021
$-2f_0$	$2f_1$	–	1.23 813	0.00 087	2.9	0.105	161	2.125	0.102	−0.00 037
$2f_0$	$3f_1$	–	10.95 270	0.00 099	3.3	0.104	203	−0.148	0.114	0.00 015
$-2f_0$	$3f_1$	–	3.67 725	0.00 114	2.8	0.108	152	1.295	0.133	0.00 054
$2f_0$	$4f_1$	–	13.38 950	0.00 097	1.8	0.105	67	1.820	0.120	−0.00 126
$-2f_0$	$4f_1$	–	6.12 023	0.00 137	1.7	0.106	57	1.765	0.148	0.00 531
$2f_0$	$5f_1$	–	15.82 902	0.00 170	1.1	0.103	26	−2.082	0.179	0.00 005
$-2f_0$	$5f_1$	–	8.55 350	0.00 189	1.3	0.101	34	0.463	0.209	0.00 037
$-2f_0$	$6f_1$	–	10.99 215	0.00 366	0.9	0.101	19	−0.578	0.322	0.00 081
$3f_0$	f_1	–	7.89 427	0.00 093	3.0	0.113	173	−0.447	0.117	−0.00 082
$3f_0$	$2f_1$	–	10.33 075	0.00 155	1.8	0.104	68	2.806	0.168	−0.00 255
$3f_0$	$3f_1$	–	12.77 310	0.00 410	0.7	0.102	11	2.485	0.272	0.00 159
$4f_0$	f_1	–	9.71 217	0.00 329	0.9	0.117	17	1.952	0.351	−0.00 188
–	–	f_i	1.96 161	0.00 257	1.6	0.100	53	1.114	0.381	0.00 000
–	f_1	f_i	4.40 172	0.00 229	0.8	0.100	14	−0.942	0.292	0.00 190
–	–	$2f_i = f_{ii}$	3.92 593	0.00 144	2.5	0.117	122	2.014	0.117	0.00 271
–	f_1	$2f_i$	6.36 320	0.00 240	1.0	0.109	23	−2.042	0.216	0.00 177
f_0	f_1	$2f_i$	8.18 505	0.00 246	0.7	0.103	11	−2.445	0.289	0.00 466
$-3f_0$	$3f_1$	$2f_i$	5.78 067	0.00 238	0.8	0.101	16	−1.855	0.319	−0.00 030
$-4f_0$	$2f_1$	$2f_i$	1.52 777	0.00 382	0.8	0.101	13	−1.957	0.248	0.00 397
$-4f_0$	$3f_1$	$2f_i$	3.95 930	0.00 167	1.4	0.124	40	−2.055	0.136	−0.00 271
$-4f_0$	$4f_1$	$2f_i$	6.39 875	0.00 193	1.4	0.109	43	0.931	0.169	−0.00 147
$-4f_0$	$5f_1$	$2f_i$	8.83 928	0.00 445	0.8	0.101	15	−2.741	0.632	0.00 085

Notes. Id: identification, f: frequency (d^{-1}), σ_f: error in frequency (d^{-1}) (1σ), A: amplitude (mmag), σ_A: error in amplitude (mmag) (1σ), Sig.: spectral significance, θ: phase, σ_θ: error in phase (1σ), Comb.err.: deviation $f - f_c$ from the numerical value for combinations $f_c = af_0 + bf_1 + cf_i$.

3.4 The largest intrinsic variations observed by MOST – an unexpected challenge

MOST was designed to detect and characterize very low amplitude stellar oscillations, down to a few μmag. AQ Leo is an exception to the MOST target list, varying over a range of a few ×0.1 mag. A common MOST data reduction procedure of correcting the data is to apply a running mean to reduce the MOST-orbit-modulated stray light signal. In this case, however, the stellar variability is large enough that this introduces a modulation because the relative contribution of the stray light variation changes with the mean brightness of the star. By fitting sky values versus instrumental magnitude, the effects of stray light can be largely removed, but the intrinsic stellar variation serves to modulate the relative contribution of the stray light to the light curve. This introduces a small artefact signal side lobe mirroring the MOST orbital frequency but reduced in amplitude compared to the intrinsic stellar signal by a factor of about 100. For example, the frequency f_1 in Table 1 will be reproduced at a frequency equal to the MOST orbital frequency minus f_1, but at a much lower amplitude.

We tested this through simulations by mimicking the raw stellar photometry by adding a constant offset to the background light curve and subsequently introducing the undeniably intrinsic stellar variability represented by the linear combinations of the first overtone f_1 and fundamental mode f_0 of AQ Leo. As suspected, in addition to the background frequencies and the aforementioned linear combinations, peaks due to beat frequencies among f_1, f_0 and the MOST orbital period appear in the amplitude spectrum. These

© 2007 The Authors. Journal compilation © 2007 RAS, MNRAS **379,** 1498–1506

frequencies are recognized and rejected in the analyses of versions of the light curve reduced with a running mean, and are not seen in reductions which do not apply this filtering technique. The MOST team is now alert to this effect for any possible future observations of large-amplitude variable stars.

3.5 Intrinsic frequencies in AQ Leo

As a result of the described procedures, we identified 42 frequencies in the AQ Leo time series intrinsic to the star. All the approaches described above led to this consistent solution. The two dominant frequencies are the first radial overtone f_1 and the fundamental radial mode f_0. Of the remaining frequencies, 32 are linear combinations of these two up to the sixth order (see the Discussion in the next section). The uncertainties of the frequencies, amplitudes and phases were estimated through extensive Monte Carlo simulations as well as through bootstrapping, as described above. The resulting uncertainties are comparable with those obtained using the formulation of Montgomery & O'Donoghue (1999). All 42 frequencies pass the conditional spectral significance test and cannot be reproduced from the background time series which contains solely instrumental signal and stray light.

The 42 frequencies include 11 which are not linear combinations of f_0 and f_1. These are $1.96\,\mathrm{d}^{-1}$, one which corresponds to its first harmonic at $3.92\,\mathrm{d}^{-1}$ (and which has a higher amplitude), and their linear combinations with f_0 and f_1. We were very cautious about these frequencies because of their proximity to integer numbers of cycles per day. The nearly continuous MOST time series does not suffer from cycle/day aliases found in ground-based single-site data due to night/day gaps, but there are subtle modulations of stray light at 1, 2, 3 and $4\,\mathrm{d}^{-1}$ due to MOST's Sun-synchronous orbit (which brings the satellite to nearly the same point over the Earth after 1 d). However, our analysis identified and rejected those artefacts at 2.00 and $4.00\,\mathrm{d}^{-1}$ present in the background measurements and did not reject the frequencies at 1.96 and $3.92\,\mathrm{d}^{-1}$, which differ from potential artefacts by more than the frequency resolution of the data set. Indeed, these frequencies are retained with high significance and signal-to-noise ratio. To stress their importance among the set of 42 frequencies, we hereafter refer to them as $f_\mathrm{i} = 1.96\,\mathrm{d}^{-1}$ and $f_\mathrm{ii} = 3.92\,\mathrm{d}^{-1}$.

The frequencies, their amplitudes, phases and uncertainties are listed in Table 1. The amplitude spectrum showing these frequencies is plotted in Fig. 2.

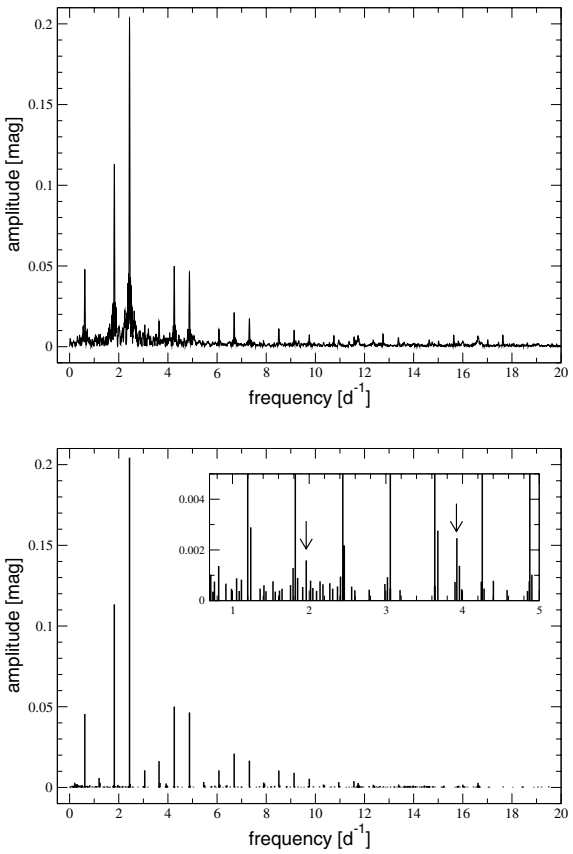

Figure 2. Upper panel: the amplitude spectrum of the AQ Leo light curve. Most of the linear combinations of f_0 and f_1 can be identified by eye. Lower panel: the amplitude spectrum for frequencies identified by SIGSPEC. The inset is a close-up of the low frequency range containing f_i and f_ii.

4 DISCUSSION

4.1 Combination frequencies of the two dominant modes

The MOST photometry has revealed an unprecedented number of frequencies (42) in AQ Leo. JW77 first detected the first radial overtone and fundamental radial modes in this star. They modelled their light curve with a double-harmonic series and by fitting different numbers of higher order terms until the standard deviation of the fitted curve was near the lower limit of the mean error of a single observation. JW77 arrived at a fit with 14 frequencies, of which 12 are combination frequencies of the two dominant modes. Of our 42 frequencies, 32 are linear combinations of those same modes.

The numerical combinations can be obtained arithmetically in Table 1 but are much easier to see when the frequencies are plotted in 'échelle' diagrams like Fig. 3. These diagrams have the same form as the échelle diagrams used in asteroseismology to highlight the asymptotic distribution of non-radial p modes. The frequencies

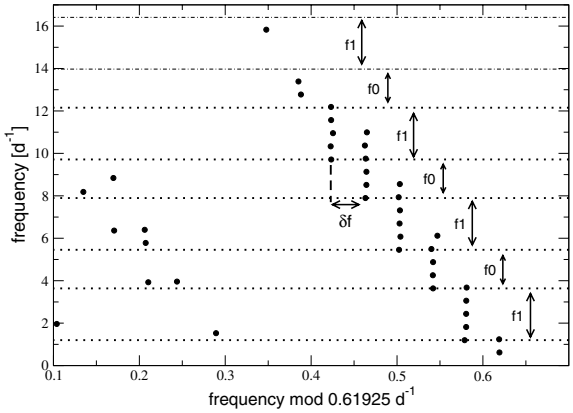

Figure 3. Graphical presentations of the linear combinations of the two dominant modes in AQ Leo, in the form of 'echelle' diagrams. The observed frequencies folded at the beat frequency $f_1 - f_0 = 0.61925\,\mathrm{d}^{-1}$ show differences of $\delta f = 3f_1 - 4f_0$ in a regular pattern alternating by f_0 and f_1.

are folded modulo a common frequency spacing on the x-axis and plotted at their original values on the y-axis. In the case of the MOST AQ Leo frequencies (and for RRd frequencies in general), the frequencies align clearly in such a diagram due to their arithmetic relationships.

In Fig. 3, the points on the right-hand side of the diagram and climbing upwards to the left with regular 'jumps' are the linear

combinations of f_0 and f_1, or $if_1 + jf_0$. (For this diagram, they are written in the practical form of $kf_1 + lf_0 + m\ (f_1 - f_0)$, where i, j and k, l, m are integer numbers.) The 'jumps' in the diagram occur when the linear combinations go up by one order, and are due to the simple fact that $f_1 \bmod(\mathrm{f_1} - \mathrm{f_0}) = \mathrm{f_0} \bmod(\mathrm{f_1} - \mathrm{f_0}) \neq 0$. Hence, for every additional f_0 or f_1 in a linear combination [besides multiples of $(f_1 - f_0)$], the 'folded' (modulo) value changes. The change corresponds to $\delta f = 3\,f_1 - 4f_0 = 0.03\,879\,\mathrm{d}^{-1}$. The points at almost the same y value in the diagram show that, from this MOST data set, we were able to separate different linear combinations of f_0 and f_1 as close as $0.03\,879\,\mathrm{d}^{-1}$ to one another. The frequencies which fall in the left bottom corner of Fig. 3 are associated with the additional frequencies at 1.96 and $3.92\,\mathrm{d}^{-1}$. Note that those frequencies also follow a pattern of regular 'jumps', since we have detected linear combinations of these frequencies with f_0 and f_1. We stress that the regular patterns are merely a consequence of the arithmetic relations between the frequencies in the linear combinations.

The MOST photometry of AQ Leo opens the possibility of a detailed analysis of the properties of the combination frequencies resulting from non-linear coupling, which can be used to test hydrodynamical models of RRd stars (see Section 4.2).

The phase diagrams of the two dominant modes are shown in Fig. 4, in which the linear combinations and frequencies unrelated to the two dominant modes we find in the fit (Table 1) have been subtracted. In AQ Leo, the first overtone mode is the dominant one. It is characterized by stronger non-linear behaviour which can be seen by the more pronounced non-sinusoidal shape of its light curve in Fig. 4.

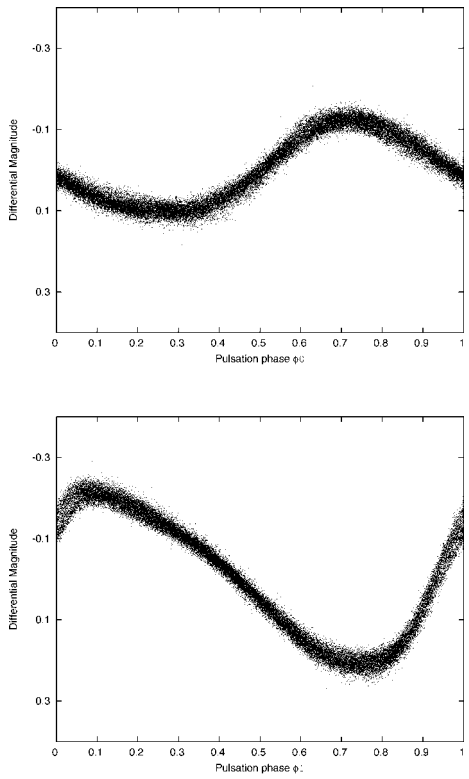

Figure 4. The deconvolved residuals of the MOST light curve of AQ Leo (after removal of combination frequencies and the additional frequencies) folded with the fundamental radial mode period P_0 (upper panel) and with the first overtone radial mode period P_1 (lower panel).

4.2 Amplitude ratios and comparison to theory

Early in the study of RRd stars, it was believed that they were in the process of switching from the fundamental radial mode to the first overtone or vice versa. Cox, Hodson & King (1980) concluded that the double-mode behaviour of AQ Leo could be explained by mode switching during its blueward or redward horizontal branch evolution. This mode-switching phase is very brief compared to the star's duration as an RR Lyrae variable – lasting only a few thousand years (Cox et al. 1980; Cox, Hodson & Clancy 1983). This is too short to account for the observed numbers of RRd stars in clusters like M15 (see Paparó et al. 1998), which suggests that the RRd stage must on average last longer than the theoretically predicted mode-switching time-scales. Feuchtinger (1998) was the first to find stable (i.e. not resulting from mode switching) double-mode behaviour in RR Lyrae models by including a time-dependent mixing length model for convection. Subsequently, convection was established by Kolláth et al. (2002) as the key player in double-mode pulsation in Cepheid and RR Lyrae models.

Even so, there is some observational evidence that the transition from a monoperiodic RR Lyrae star (RRc: redward or RRab: blueward) to a double-mode RR Lyrae star can take place over a very short time-scale. Clement & Goranskij (1999) observed a rapid mode change from RRab to RRd in the star V79 in the cluster M3 in less than a year. Buchler & Kolláth (2002) have shown that bifurcation points (characterized by changes in pulsation behaviour) exist where pulsation is no longer independent from stellar evolution. Taking this into account, the number of observed double-mode pulsators suggests that these oscillations are stable and that rapid mode switching is a relatively rare effect. Still, the true nature of double-mode pulsation in individual stars remains elusive from the observers' point of view.

If the kinetic energy switching times are only a few hundred years or less and the relative amplitude change time-scale less than a thousand years, the relative amplitudes of the two modes might be seen to change over time-scales of decades. The amplitude ratio of the first overtone to fundamental mode in AQ Leo in 1973–1975 measured by JW77 was $A_1/A_0 \simeq 2$. The amplitude ratio measured by MOST in 2005 is $A_1/A_0 \simeq 1.8$. Unfortunately, it is risky to compare our observed amplitudes and phases to those tabulated by JW77, because the MOST photometry was obtained through a wide non-standard passband while the JW77 data were obtained through a Johnson B filter.

A qualitative comparison to an RRd model (see Kovács & Buchler 1993) is presented in Figs 5 and 6. The striking similarities to the model results in the MOST light curve and resulting amplitude spectrum shows that current space-based observations are able to reach the quality of numerical simulations. Admittedly, the frequencies of the fundamental and the first overtone themselves don't match and we do not propose this model to be an accurate description of AQ Leo. The model was calculated under the unrealistic assumption of a purely radiative stellar envelope. By today's standards, more sophisticated treatments of the hydrodynamic equations (including convection) in the calculations are more reasonable (Kolláth & Buchler 2001). Still, the predicted relative amplitudes of the various linear combinations of f_0 and f_1 behave in close agreement with our observations up to very high order. As such, observations of the quality presented in this paper should be considered to be a tool of validation for the non-linear pulsational behaviour of modern RRd models. The observed frequencies, their amplitudes and phases can even be a testing ground for the development of hydrodynamical models of RRd stars including non-radial pulsations.

© 2007 The Authors. Journal compilation © 2007 RAS, MNRAS **379,** 1498–1506

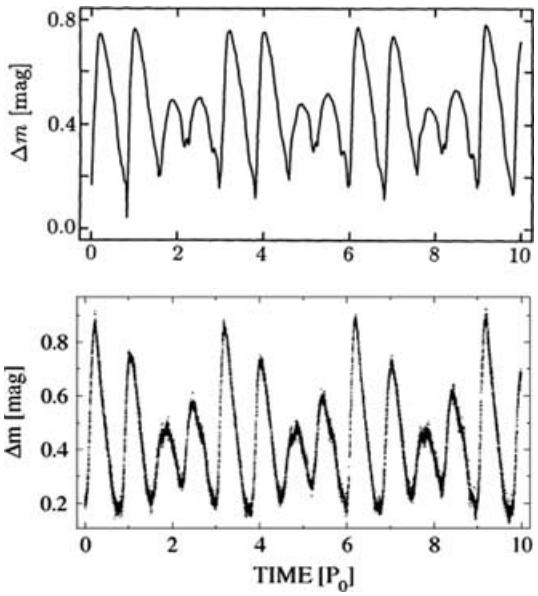

Figure 5. Comparing light curves from a computer and from space. A segment of the theoretical light curve of a purely radiative RRd star, taken from Kovács & Buchler (1993) covering 10 cycles of the fundamental mode period in their model [upper panel – reproduced by permission of the American Astronomical Society (AAS)]. A segment of the MOST light curve of AQ Leo spanning the same amount of time, shown at the same scale (lower panel). It is now possible to obtain data which is sampled as thoroughly and with noise levels comparable to time-resolved model calculations.

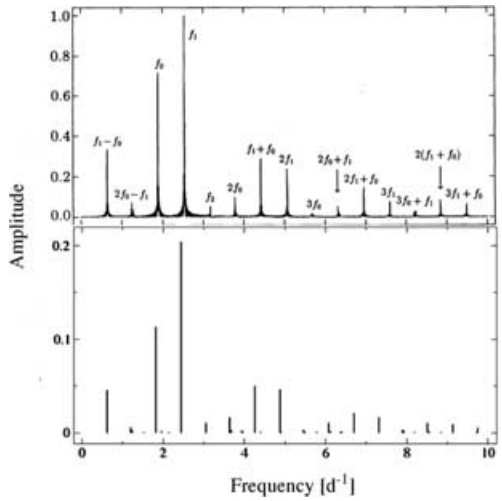

Figure 6. Amplitude spectra of the model light curve from Fig. 5, taken from Kovács & Buchler (1993) (upper panel – reproduced by permission of the AAS) and the MOST photometry in the same frequency range (lower panel). The relative amplitudes compare quite well to our findings.

4.3 Period changes?

Basic pulsation physics predicts that an increase in the fundamental mode period would be accompanied by an increase in the first overtone mode period, reflecting an increase in the mean stellar density. Paparó et al. (1998) studied period changes in RRd stars in M15 and found that the rate of period change for the fundamental radial mode is significantly larger than for the first overtone. For most of the stars in their sample, the ratio P_0/P_1 is increasing. They found the period changes of the fundamental modes of the RRd stars were mostly negative, while for the first overtone, both positive and negative changes were seen. The most striking result by Paparó et al. (1998) is the measurement of period changes of different sign for the fundamental and first overtone modes. This suggests, as for the δ Scuti pulsators, that the period changes may not be simply linked to an RR Lyrae star's evolution in the HR diagram.

The uncertainties in the frequencies in Table 1 are slightly too large, given that the MOST time series spans only about 34 d, to measure reliably the predicted evolutionary period changes in the 30 yr between the MOST and JW77 observing runs. However, JSW82 deduced that there was a sudden increase of the period of the first overtone of AQ Leo in the early 1970s, by comparing re-evaluated JW77 photometry to archived data dating back to 1929. It is possible that there have been other period changes in AQ Leo unrelated to the evolution of the mean density of the star.

Therefore, we compared the periods from the MOST photometry to the values reported in JSW82. (We cannot perform a meaningful O–C analysis due to the complexities of the light curves.) Our results yield evidence for frequency changes in AQ Leo since the JW77 observations outside the 1σ uncertainties: fundamental mode,

$$\Delta f_0 = -0.00005 \pm 0.00002\,\mathrm{d}^{-1},$$

and first overtone,

$$\Delta f_1 = +0.00007 \pm 0.00001\,\mathrm{d}^{-1}.$$

While the change of the fundamental frequency is consistent with zero within the 3σ confidence limits, the non-zero positive change of the first overtone is highly significant. Interestingly, the value of f_1 we obtained from the MOST data matches that proposed in JSW82 to satisfy an O–C diagram covering the data obtained from 1929 up to right before the abrupt period change in the 1970s. Our results fit their findings to within the 1σ uncertainties. This hints that the period change in the 1970s was a short-lived event.

Consequently, notwithstanding the higher uncertainties, we obtain a slightly different period ratio than that of JSW82, namely $P_1/P_0 = 0.74\,602 \pm 0.00\,002$ compared to $0.746\,063 \pm 0.000\,003$. This does not significantly disagree with the theoretical result of Cox et al. (1980), who calculated that the fundamental mode period and the period ratio of 0.746 can be explained if AQ Leo has a homogeneous composition typical of Population II and a mass of $0.65\,\mathrm{M}_\odot$. More recent calculations (Kolláth, private communications) indicate, however, that a mass $>0.7\,\mathrm{M}_\odot$ is likely to be more accurate. When compared to the results of Szabó, Kolláth & Buchler (2004), our values match the sequence with $M = 0.71\,\mathrm{M}_\odot$, $L = 60\,\mathrm{L}_\odot$ and very low metallicity.

4.4 New modes in AQ Leo?

RR Lyrae stars have long been considered prototypes of radially pulsating stars. Two types of RR Lyrae stars show multiperiodic behaviour: Blazhko stars and double-mode stars, like AQ Leo. The former are characterized by the Blazhko effect (see Kovács 2001; Kolenberg 2004), which is a periodic modulation of the amplitude and/or phase of the light curve on time-scales of a few up to hundreds of days. In the Fourier spectra of such stars, additional frequencies occur close to the dominant frequency which is identified with a radial mode. If these frequencies correspond to pulsation modes in the star, they must be non-radial modes. van Hoolst, Dziembowski & Kawaler (1998) showed that there is a dense spectrum of non-radial modes which have lower moments of inertia (and hence are more easily excited) in the vicinity of the radial mode frequencies in RR Lyrae stars.

The MOST observations of AQ Leo are the first in which additional frequencies besides the fundamental radial mode, the first overtone radial mode and their linear combinations are detected. The two additional frequencies are $f_{\rm i} \simeq 1.96\,{\rm d}^{-1}$ and $f_{\rm ii} \simeq 3.92\,{\rm d}^{-1}$. (Linear combinations of these frequencies with the known radial modes are also found in the data, see also Fig. 3.) The amplitude ratio of $f_{\rm i}$ to $f_{\rm ii}$ is 0.64 ± 0.08.

Judging from the period ratios alone, $f_{\rm ii}$ ($\simeq 2f_{\rm i}$) could be the third radial overtone (Kolláth, private communications). If it is a strange mode (essentially an acoustic surface mode; see Buchler, Yecko & Kolláth 1997b), $f_{\rm i}$ could then be a non-radial mode in a resonant (2:1) interaction with the third overtone. This scenario has been considered theoretically in studies of pulsational resonance (Buchler, Goupil & Hansen 1997a), supporting our argument. If we are indeed witnessing resonance of a non-radial and a radial mode, it is the higher frequency which must correspond to $\ell = 0$ due to parity considerations. The frequencies match the resonance within the uncertainties (see Table 1). In case of a mismatch, the resonance cannot be locked. The fact that we see significant amplitudes at both frequencies may suggest that AQ Leo is in a fleeting state of mode transition. Previous calculations by Buchler et al. (1997b) predicted that if strange modes are present, they should correspond to higher overtones than the third. Our new frequencies are more consistent with the third overtone, so models matched more closely to AQ Leo are necessary to compare with the MOST observations.

The frequency $f_{\rm i}$ – close to the radial fundamental mode – is also reminiscent of the additional frequencies seen in Blazhko stars. While the nature of the additional frequencies in AQ Leo, as well as in Blazhko stars (see e.g. Kolenberg et al. 2003), must still be thoroughly investigated, there is increasing evidence that some RR Lyrae stars pulsate 'beyond radial modes' (e.g. Kiss et al. 1999; Clement & Rowe 2000). Our observations represent the first detection of additional modes in an RRd star.

5 WHERE DO WE GO FROM HERE?

Nearly continuous MOST photometry of AQ Leo spanning about 34.4 d and with high photometric precision have provided (1) accurate Fourier components of the known radial fundamental and first overtone modes in this star; (2) an unprecedented number of 32 combination frequencies of these modes; (3) evidence for non-evolutionary changes in the periods of the fundamental and (even more strongly) the first overtone mode and (4) additional frequencies which can only be plausibly explained by other modes which have never been seen before in AQ Leo, or in any RRd star until now. What are the next steps forward?

Observationally, it will be very difficult – perhaps impossible – to obtain a light curve of longer time coverage and better precision than the MOST photometry presented here in the near future. The star will not be accessible to the CoRoT (Convection Rotation and planetary Transits) and Kepler space missions, nor will ground-based photometric campaigns reach what MOST has achieved for AQ Leo for some time to come. If AQ Leo is re-observed by MOST in the coming years, it could provide a reliable measurement of the change in amplitude ratio of the radial fundamental and overtone modes in the MOST bandpass, to test theories of mode switching and evolution in this star. Furthermore, further evidence for the period changes may be established.

New MOST photometry may lead to the detection of even more frequencies (depending on the behaviour of AQ Leo) but it will not be possible to improve the frequency resolution of the current data set dramatically. Time-resolved high-resolution spectroscopy to look for evidence of non-radial pulsation in the spectral line profile shapes would be highly desirable for this star. Unfortunately, AQ Leo is quite faint ($V \sim 12.6$), so spectroscopy of sufficient wavelength resolution and high signal-to-noise ratio are beyond reach of instruments which could monitor the star at a sufficient cadence for many weeks.

The immediate path to better understanding of AQ Leo is theoretical modelling of the frequency spectrum identified in the existing MOST photometry. The potential of the combination frequencies to test hydrodynamical models can now be fully exploited thanks to the very precise MOST data.

ACKNOWLEDGMENTS

We would like to thank Zoltan Kolláth and Geza Kovács for their valuable contributions to the discussion. MG, TK, WWW (Project number P17580-N02) and KK (Project number P17097-N02) have received financial support by the Austrian Fonds zur Förderung der wissenschaftlichen Forschung. JMM, DBG, AFJM, SR, DS and GAHW acknowledge funding from the Natural Sciences & Engineering Research Council (NSERC), Canada. RK is supported by the Canadian Space Agency (CSA).

REFERENCES

Alcock C. et al., 2000, ApJ, 542, 257
Buchler J. R., Kolláth Z., 2002, ApJ, 573, 324
Buchler J. R., Goupil M.-J., Hansen C. J., 1997a, A&A, 321, 159
Buchler J. R., Yecko P. A., Kolláth Z., 1997b, ApJ, 326, 669
Cameron C. et al., 2006, Commun. Asteroseismol., 148, 57
Clement C. M., Goranskij V. P., 1999, ApJ, 513, 767
Clement C. M., Rowe J. F., 2000, AJ, 120, 2579
Clement C. M., Kinman T. D., Suntzeff N. B., 1991, ApJ, 372, 273
Clement C. M., Jankulak M., Simon N. R., 1992, ApJ, 395, 192
Cox A. N., Hodson S. W., King D. S., 1980, ApJ, 236, 219
Cox A. N., Hodson S. W., Clancy S. P., 1983, ApJ, 266, 94
Feuchtinger C., 1998, A&A, 337, L29
Hoffmeister C., 1944, Astron. Nachr., 274, 176
Jerzykiewicz M., Wenzel W., 1977, Acta Astron., 27, 35 (JW77)
Jerzykiewicz M., Schult R. H., Wenzel W., 1982, Acta Astron., 32, 357 (JSW82)
Kallinger T., Reegen P., Weiss W. W., 2007, A&A, submitted
Kiss L. L., Csák B., Thomson J. R., Vink'o J., 1999, A&A, 345, 149
Kolenberg K., 2004, Commun. Asteroseismol., 144, 5
Kolenberg K., Aerts C., Fokin A., Dziembowski W., Chadid M., Gillet D., 2003, in Sterken Ch., ed., ASP Conf. Ser. Vol. 292, Interplay of Periodic, Cyclic and Stochastic Variability in Selected Areas of the H–R iagram. Astron. Soc. Pac., San Francisco, p. 171
Kolláth Z., Buchler J. R., 2001, in Takeuti M., Sasselov D. D., eds, Astrophysics and Space Science Library Vol. 257, Stellar Pulsation – Nonlinear Studies. Kluwer, Dordrecht, p. 29
Kolláth Z., Buchler J. R., Szabó R., Csubry Z., 2002, A&A, 385, 932
Kovács G., 2001, in Takeuti M., Sasselov D. D., eds, Astrophysics and Space Science Library Vol. 257, Stellar Pulsation – Nonlinear Studies. Kluwer, Dordrecht, p. 61
Kovács G., Buchler J. R., 1993, ApJ, 404, 765
Kovács G., Buchler J. R., Marom A., 1991, A&A, 252, 27
Lenz P., Breger M., 2005, Commun. Asteroseismol., 146, 53
Montgomery M., O'Donoghue D., 1999, Delta Scuti Newsl., 13, 45
Oaster L., Smith H. A., Kinemuchi K., 2006, PASP, 841, 405
Paparó M., Saad S. M., Szeidl B., Kolláth Z., Abu Elazm M. S., Sharaf M. A., 1998, A&A, 332, 102

Reegen P., 2005, in Zverko J., Ziznovsky J., Adelman S. J., Weiss W. W., eds, Proc. IAU Symp. 224, The A-Star Puzzle. Cambridge Univ. Press, Cambridge, p. 791
Reegen P., 2007, A&A, 467, 1353
Reegen P. et al., 2006, MNRAS, 367, 1417
Rowe J. F. et al., 2006a, Mem. Soc. Astron. Italia, 77, 282
Rowe J. F. et al., 2006b, Commun. Asteroseismol., 148, 34
Saio H. et al., 2006, ApJ, 650, 1111
Smith H. A., 1995, RR Lyrae Stars. Cambridge Univ. Press, Cambridge
Szabó R., Kolláth Z., Buchler J. R., 2004, A&A, 425, 627
Szeidl B., 1988, in Kovács G., Szabados L., Szeidl B., eds, Multimode Stellar Pulsations. Konkoly Observatory, Kultura, p. 45
van Hoolst T., Dziembowski W. A., Kawaler S. D., 1998, MNRAS, 297, 536
Walker G. A. H. et al., 2003, PASP, 115, 1023
Wall J. V., Jenkins C. R., 2003, Practical Statistics for Astronomers. Cambridge Univ. Press
Wenzel W., 1961, Veroeffentlichungen der Sternwarte in Sonneberg, 5, 84

This paper has been typeset from a TEX/LATEX file prepared by the author.